

Hybrid anisotropic pentamode mechanical metamaterial produced by additive manufacturing technique

Mohammadi, Kaivan; Movahhedy, Mohammad R.; Shishkovsky, Igor; Hedayati, Reza

DOI

[10.1063/5.0014167](https://doi.org/10.1063/5.0014167)

Publication date

2020

Document Version

Final published version

Published in

Applied Physics Letters

Citation (APA)

Mohammadi, K., Movahhedy, M. R., Shishkovsky, I., & Hedayati, R. (2020). Hybrid anisotropic pentamode mechanical metamaterial produced by additive manufacturing technique. *Applied Physics Letters*, 117(6), Article 061901. <https://doi.org/10.1063/5.0014167>

Important note

To cite this publication, please use the final published version (if applicable).
Please check the document version above.

Copyright

Other than for strictly personal use, it is not permitted to download, forward or distribute the text or part of it, without the consent of the author(s) and/or copyright holder(s), unless the work is under an open content license such as Creative Commons.

Takedown policy

Please contact us and provide details if you believe this document breaches copyrights.
We will remove access to the work immediately and investigate your claim.

Hybrid anisotropic pentamode mechanical metamaterial produced by additive manufacturing technique

Cite as: Appl. Phys. Lett. **117**, 061901 (2020); <https://doi.org/10.1063/5.0014167>

Submitted: 18 May 2020 . Accepted: 22 July 2020 . Published Online: 11 August 2020

Kaivan Mohammadi, Mohammad R. Movahhedy, Igor Shishkovsky , and Reza Hedayati 



View Online



Export Citation



CrossMark

ARTICLES YOU MAY BE INTERESTED IN

[Hybrid metamaterials enable multifunctional manipulation of mechanical waves on solid-fluid interfaces](#)

Applied Physics Letters **117**, 061902 (2020); <https://doi.org/10.1063/5.0021302>

[Light-emitting diodes with AlN polarization-induced buried tunnel junctions: A second look](#)

Applied Physics Letters **117**, 061104 (2020); <https://doi.org/10.1063/5.0015097>

[Artificial resonant crystals for hydroelastic waves](#)

Applied Physics Letters **117**, 063701 (2020); <https://doi.org/10.1063/5.0018823>



HIDEN
ANALYTICAL

Instruments for Advanced Science

Gas Analysis



- dynamic measurement of reaction gas streams
- catalysis and thermal analysis
- molecular beam studies
- dissolved species probes
- fermentation, environmental and ecological studies

Surface Science



- UHV TPD
- SIMS
- end point detection in ion beam etch
- elemental imaging - surface mapping

Plasma Diagnostics



- plasma source characterization
- etch and deposition process reaction kinetic studies
- analysis of neutral and radical species

Vacuum Analysis



- partial pressure measurement and control of process gases
- reactive sputter process control
- vacuum diagnostics
- vacuum coating process monitoring

Contact Hiden Analytical for further details:
W www.HidenAnalytical.com
E info@hiden.co.uk

CLICK TO VIEW our product catalogue

Hybrid anisotropic pentamode mechanical metamaterial produced by additive manufacturing technique

Cite as: Appl. Phys. Lett. **117**, 061901 (2020); doi: [10.1063/5.0014167](https://doi.org/10.1063/5.0014167)

Submitted: 18 May 2020 · Accepted: 22 July 2020 ·

Published Online: 11 August 2020



View Online



Export Citation



CrossMark

Kaivan Mohammadi,¹ Mohammad R. Movahhedy,¹ Igor Shishkovsky,²  and Reza Hedayati^{3,a)} 

AFFILIATIONS

¹Additive Manufacturing Lab (AML), Department of Mechanical Engineering, Sharif University of Technology, Azadi Avenue, 11365-11155 Tehran, Iran

²Center for Design, Manufacturing and Materials, Skolkovo Institute of Science and Technology, 3 Nobel Str., 121205 Moscow, Russia

³Novel Aerospace Materials Group, Faculty of Aerospace Engineering, Delft University of Technology (TU Delft), Kluyverweg 1, 2629 HS Delft, the Netherlands

^{a)}Author to whom correspondence should be addressed: r.hedayati@tudelft.nl and rezahedayati@gmail.com.

Tel.: +31 (0)15 27 88777

ABSTRACT

Pentamode metamaterials are a type of extremal designer metamaterials, which are able to demonstrate extremely high rigidity in one direction and extremely high compliance in other directions. Pentamodes can, therefore, be considered as building blocks of exotic materials with any arbitrarily selected thermodynamically admissible elasticity tensor. The pentamode lattices can then be envisioned to be combined to construct intermediate extremal materials, such as quadramodes, trimodes, and bimodes. In this study, we constructed several primary types of anisotropic pentamode lattices (with midpoint positioning of 10%, 15%, 20%, 25%, 30%, 35%, and 42% of the main unit cell diagonal) and then combined them mutually to explore the dependence of elastic properties of hybrid pentamodes on those of individual constructing lattices. Several anisotropic individual and hybrid pentamode lattice structures were produced using the MultiJet Additive Manufacturing technique and then mechanically tested under compression. Finite element models were also created using the COMSOL Multiphysics package. Two-component hybrid pentamode lattices composed of individual lattices with extensively different (as large as two orders of magnitudes) B/G ratios were constructed and analyzed. It was demonstrated that it is possible to design and construct composite intermediate extremal materials with arbitrary eigenvalues in the elastic tensor. It is concluded that the elastic E , shear G , and bulk moduli B of the hybrid structure are the superpositions of the corresponding moduli of the individual lattice structures. Poisson's ratio ν of the hybrid pentamode structure equals that of individual structure with higher Poisson's ratio. The yield stress σ_y of the hybrid pentamode lattice structure depends on the elastic moduli of the constructing lattice structures, as well as the yield stress of the weaker lattice structure.

Published under license by AIP Publishing. <https://doi.org/10.1063/5.0014167>

Mechanical metamaterials are rationally designed lattices that demonstrate exotic mechanical properties such as negative compressibility,¹ negative Poisson's ratio,² double negativity,³ and fluid-like behavior,^{4–7} which are not found or are very rare in nature. The latter, commonly known as pentamode metamaterials, are a type of extremal designer metamaterials,^{5,8} which are able to demonstrate extremely high rigidity in one direction and extremely high compliance in other directions. This has led to the proposition of pentamodes having bulk moduli orders of magnitude greater than their shear moduli.⁹ This has earned pentamodes the name “metafluids” as fluids also have very small shear resistivity while they demonstrate very high

incompressibility levels.⁷ However, unlike fluids, pentamodes have the capability of being designed to have characteristics such as stability, inhomogeneity, and anisotropy.¹⁰

Pentamode metamaterials were first theoretically introduced by Milton and Cherkov in 1995,¹¹ but they were not experimentally realized until very recently⁹ thanks to extensive developments in additive manufacturing (AM) technologies. Mathematically speaking, pentamodes are materials that have one extremely high pressure-type eigenvalue in their elasticity tensor, while the values of other eigenvalues in the elasticity tensor are negligible. Pentamodes can, therefore, be considered as building blocks of exotic materials with any

arbitrarily selected thermodynamically admissible elasticity tensor. The pentamode lattices can then be envisioned to be combined to construct intermediate extremal materials, such as quadramodes, trimodes, and bimodes.¹¹ Even though several designs have been proposed for pentamodes,^{12–15} the most common pentamode metamaterials are face-center cubic (fcc) diamond-shaped lattice structures made up of double-cone linkages, the cones being attached to each other at their larger diameter D at the midpoint of the linkage.^{6,16–20} If the smaller diameter of the pentamode, d , is chosen small enough (i.e., $d/a < 4\%$,^{5,7} where a is the unit cell size), the effect of the larger diameter size on the elastic modulus becomes negligible and the smaller diameter determines the macro-scale properties of the structure.⁷

In their early work, Milton and Cherkaev¹¹ suggested creating holes in the linkages or converting vertices into a cluster of vertices to avoid interpenetration of individual pentamode lattices, which are used to create intermediate extremal materials. Another approach to avoid the intersection of linkages is to combine pentamodes with anisotropic microgeometries. In that way, while the microgeometry of each individual pentamode lattices is chosen to accommodate to its corresponding pre-defined elasticity tensor, both lattices can be combined in such a way that they do not intersect with each other, therefore maintaining their initial design intact. One way of making a pentamode metamaterial anisotropic is to move the midpoint P at an initial position of $P = (0.75a, 0.75a, \text{ and } 0.25a)$ along the main diagonal of the unit cell [Fig. 1(d)] in such a way that its initial distance from the vertex is changed from 25% L to any other distance in the range of 0 and 50% L , where $L = \sqrt{3}a$ is the length of the main diagonal of the unit cell.

While anisotropy in the design of pentamodes has been previously studied acoustically in Refs. 4 and 21, making composites out of

individual pentamode lattices and the effect of elastic properties, such as elastic modulus, yield stress, and Poisson's ratio of the primary individual lattices on the elastic properties of the hybrid structure, have never been studied before. Moreover, in the work conducted in Refs. 4 and 21, only elastic and bulk moduli can be extracted from the acoustic results of anisotropic pentamodes. In the current work, yield stress, Poisson's ratio, shear modulus, and relative density, which all become practical in real applications of pentamode metamaterials, will all be studied as well. More importantly, the direction of the wave propagated inside the metamaterial in Refs. 4 and 21 [i.e., direction (1,1,1)] was different from the direction in which mechanical properties in this work have been obtained [i.e., direction (1,0,0)] and which is the direction for which mechanical properties are usually obtained in the works in the field.^{7,9,10,16–18,22}

In this study, we aim to construct several types of anisotropic pentamodes and then to combine them mutually to explore the dependence of the elastic properties (elastic modulus, shear modulus, bulk modulus, Poisson's ratio, and yield stress) of hybrid pentamodes on the elastic properties of individual constructing pentamode lattices. The influence of midpoint positioning on the elastic properties of anisotropic pentamode lattices will be studied and discussed. The lattices will be manufactured and tested experimentally. Static and dynamic simulations will also be carried out to study the mechanical properties of a larger range of anisotropic pentamodes and their hybrid constructs.

In this study, the small diameter $d = 300 \mu\text{m}$ and the large diameter $D = 1100 \mu\text{m}$ were used in all the models. The unit cell size was also kept constant $a = 8 \text{ mm}$. We chose seven particular positions for P with distances from the vertex of 10% L , 15% L , 20% L , 25% L , 30% L , 35% L , and 42% L (Fig. 1). Finite element (FE) models were created using the COMSOL Multiphysics package (Stockholm, Sweden). All the FE models were lattices made up of $5 \times 5 \times 5 = 125$ unit cells, as demonstrated in Fig. 1. The models were discretized using around 10^6 tetrahedral elements. A mesh sensitivity analysis was performed, and the numerical result converged for element sizes smaller than $20 \mu\text{m}$ at diameter d and at $140 \mu\text{m}$ at diameter D (see Figs. S1 and S2 in the supplementary material for further information). MUMPS static solver in COMSOL was used to solve continuum mechanics equations. Linear elastic material model with mechanical properties of the constituent polymeric material ($E_s = 1.528 \text{ GPa}$, $\sigma_{ys} = 42.6 \text{ MPa}$, $\nu_s = 0.4$, $\rho_s = 1020 \text{ kg/m}^3$) was implemented, and a stepwise (in 10 steps) uniform displacement of $1010 \mu\text{m}$ was applied on the top side of the lattice structure. The lowermost nodes of the lattice structure were constrained in all the directions, and the uppermost nodes of the lattice structure were only allowed to move in the loading direction. To obtain numerical yield stress values, stress-strain curves were also necessary. Therefore, dynamic analyses by considering plasticity evolution in the constituent material were carried out. For the dynamic solution, a bilinear perfectly plastic material model (see Fig. S8 in the supplementary material) was implemented.

Three of the anisotropic pentamode designs with midpoint positionings of 15% L , 25% L , and 42% L were selected for AM and mechanical testing (Fig. 2). All the specimens were fabricated using a Projet 3500 HD Max 3D printer (3D SYSTEMS, SC, US). 3D SYSTEMS' proprietary VisiJet M3 Crystal polymer was used for manufacturing the body of the lattice structure, and a pure VisiJet S300 wax was used as the support material to hold the overhanging

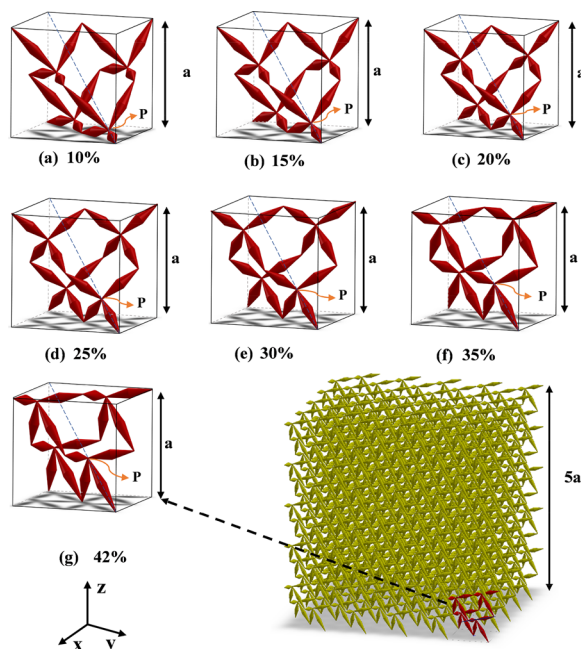


FIG. 1. Anisotropic unit cells of pentamode metamaterial with P positioning from 10% to 42%.

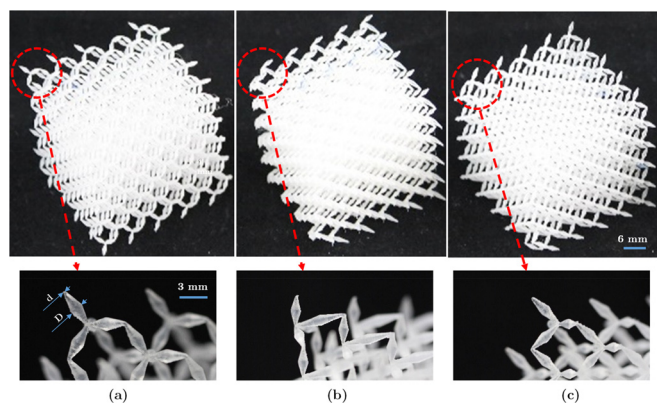


FIG. 2. Images of the specimens manufactured with midpoint positioning of (a) $P = 25\%$, (b) $P = 42\%$, and (c) $P = 15\%$.

parts, which was removed after the printing process by heating the samples up to $60\text{ }^{\circ}\text{C}$. All the specimens had good production quality, and the maximum surface roughness R_a was less than $2\text{ }\mu\text{m}$ (see also Table I). In addition, a hybrid pentamode metamaterial with two constituting pentamode lattices with midpoint positionings of 15% L and 42% L was manufactured (Fig. 3) using the same manufacturing parameters. In order to avoid free movement of the two lattices with respect to each other, the two lattices were softly connected to each other by means of two very thin ($200\text{ }\mu\text{m}$ in diameter) bars printed on two opposite edges of the lower-most surface of the specimen.

An INSTRON 5969 servo mechanical testing machine with an INSTRON 2580–500N load cell was used to load the specimens under uniaxial compressive loads with a displacement rate of 5 mm/min . The elastic properties of the structures (elastic modulus, yield stress, and Poisson’s ratio) were calculated from the obtained linear regime of load–displacement curves in accordance with the ISO standard 13314:2011. The properties were then normalized using the mechanical properties of the constituent material ($E_s = 1.528\text{ GPa}$ and $\sigma_{ys} = 42.6\text{ MPa}$). The stress–strain curves of all the lattices are provided in Fig. S3 of the supplementary material, and the stress–strain curve of the constituent material is provided in Fig. S8 of the supplementary material. Relative density is defined as the ratio of the density of a lattice structure to that of the constituent material. Experimental relative density was measured by the dry-weighing method, and the numerical relative density was calculated by dividing the volume occupied by the constituent material in a unit cell to the volume of the whole unit cell.

Even though there are several methods developed for obtaining bulk modulus of solid materials,²³ there is no standard known for the hydrostatic compression of open-cell foams (which are, in essence,

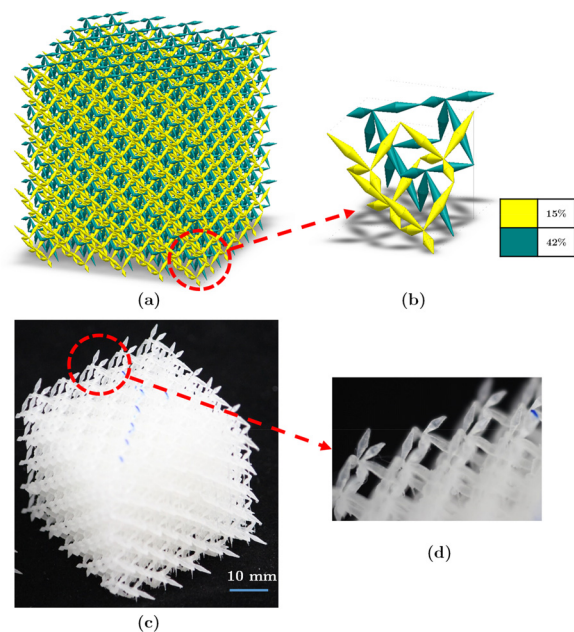


FIG. 3. (a) Lattice and (b) a unit cell of a structure combined of two pentamode metamaterials with 15% and 42% midpoint positionings. (c) and (d) The manufactured hybrid pentamode metamaterial.

similar to pentamode metamaterials as pentamodes are also open-cell and allow for the permeability of fluids).²⁴ In their work, Moore *et al.*²⁴ have developed a test apparatus for testing bulk modulus in open cell foams, which is out of the scope of this study. Performing bulk modulus experiments on pentamodes is very complex, and that is why in many works^{9,10} conducted on the bulk modulus of pentamode metamaterials, the bulk modulus is calculated indirectly using formulas and measured elastic modulus rather than performing experiments dedicated for bulk modulus. Regarding shear modulus, the setup required for shear testing was not available. However, the validation of numerical results for elastic modulus, yield stress, and Poisson’s ratio in Fig. 4 demonstrates the reliability of the numerical models and, thus, the computational values for shear modulus and bulk modulus.

All the physical and mechanical properties obtained from experimental tests and numerical models are in good agreement with each other. The maximum differences between the numerical and experimental values for relative density, elastic modulus, Poisson’s ratio, and yield stress are 16.7% , 8.1% , 29.9% , and 21.8% , respectively (Fig. 4).

As expected, the variation of the relative density μ with respect to its diagonal location is almost symmetrical and varies in a small range

TABLE I. Geometrical characteristics of different specimens manufactured.

Specimen	$d\text{ (}\mu\text{m)}$	$D\text{ (}\mu\text{m)}$	$h_1\text{ (}\mu\text{m)}$	$h_2\text{ (}\mu\text{m)}$	Surface roughness,	
					$R_a\text{ (}\mu\text{m)}$	$R_z\text{ (}\mu\text{m)}$
$15\% \text{ L}$	307 ± 7	1108 ± 13	2040 ± 36	4040 ± 16	1.34	12.14
$25\% \text{ L}$	305 ± 9	1116 ± 15	3366 ± 49	3323 ± 41	1.06	13.31
$42\% \text{ L}$	304 ± 8	1112 ± 18	5040 ± 71	3201 ± 14	1.63	9.56

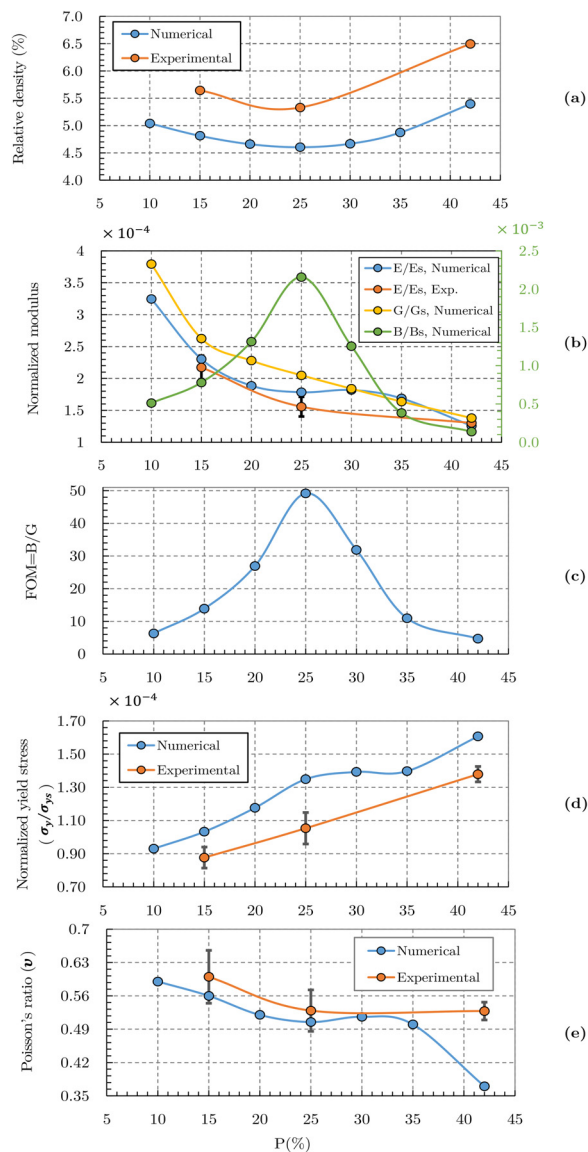


FIG. 4. Variation of (a) relative density, (b) normalized elastic modulus, (c) FOM, (d) normalized yield stress, and (e) Poisson's ratio with respect to midpoint positioning.

($0.046 < \mu < 0.054$). As seen in Figs. 4(b) and 4(e), by moving the midpoint from the vertex (10% L) toward the centroid (42% L) of the unit cell, there is a continuous decrease in the normalized elastic modulus (from 3.25×10^{-4} to 1.26×10^{-4} , i.e., 61% decrease), normalized shear modulus (from 3.79×10^{-4} to 1.38×10^{-4} , i.e., 64% decrease), and Poisson's ratio (from 0.59 to 0.37, i.e., 37% decrease). For the case of yield stress, the normalized yield stress steadily increases from 0.93×10^{-4} (at 10% L) to 1.61×10^{-4} (at 42% L). Analytical study demonstrated that for smaller diameter, larger diameter, and strut length ranges considered in this study (i.e., $d = 300 \mu\text{m}$, $D = 1100 \mu\text{m}$, and $0.1L < l < 0.5L$), if the strut is purely stretched for δ , the strain energy stored in the struts is at least two orders of

magnitude larger than that when the strut is purely bent for δ . Stress analysis in the struts demonstrated that as the midpoint position changes from the vertex towards the centroid, the main type of load sustained by the struts changes from compression to bending, which contributes to a decrease in the elastic modulus. Inversely, the described increase in flexibility and bending presence in the struts of the structure as a result of the change in the midpoint positioning from the vertex toward the centroid contributes to an increase in yield strength.

On the other hand, normalized bulk modulus has a bell-shaped curve with a peak of 2.1×10^{-3} at 25% L and a minimum value of 1.4×10^{-4} at 42% L [Fig. 4(b)]. Accordingly, the ratio B/G (also known as figures-of-merit, FOM) has a bell-shaped curve with a peak point of 50 at 25% L and a minimum of ≈ 3 at 10% L and 42% L [Fig. 4(c)]. Analysis of numerical results demonstrated that in the case of 25% L, and under triaxial stress, all the struts go under pure axial contraction (with no lateral deformation). As the positioning of the midpoint is varied toward the lower or higher ends of the spectrum (i.e., respectively, 10% L and 42% L), bending takes a larger role in the total deformation of the struts and, therefore, the structure as a whole, which leads to a bell shape in the bulk modulus curve with its maximum point at 25% L.

The value of Poisson's ratio is in the range of 0.5–0.6 for most of the range of midpoint positioning. The only exception is the case of 42% L, in which Poisson's ratio drops suddenly to 0.36. At 42% L midpoint positioning, two of the struts become horizontal and contribute very little to lateral deformation of the unit cell, which leads to a huge decrease in Poisson's ratio.

As for the case of hybrid pentamode metamaterial, the differences between the numerical and experimental values of relative density, elastic modulus, Poisson's ratio, and yield stress were 22.1%, 2.7%, 8.1%, and 23.4%, respectively (experimental results being: $\mu = 0.131$, $E = 545 \text{ kPa}$, $\nu = 0.507$, and $\sigma_y = 12.87 \text{ kPa}$). The relative density, elastic modulus, Poisson's ratio, and yield stress values of FE hybrid models constructed from individual lattice structures with different %L are demonstrated in Fig. 5, and the values are listed in Table S1 in the supplementary material. As for the relative density, it was expected that the relative density of the hybrid structure is the summation of the relative density of each individual lattice structures. This is confirmed since the expected and numerical surfaces have very similar topologies and both lie in the range of 0.0921 and 0.1079 [Figs. 5(a) and S6(a) in the supplementary material]. As for the elastic, shear and bulk moduli, a similar superposition hypothesis was expected as the stiffness of the whole hybrid structure originates from the stiffness of the individual structures, and, as a result, the hybrid structure can be considered as two separate structures working in parallel and, thus, each taking part of the load. The hypothesis was confirmed by numerical results, and, as it can be observed in Figs. 5(b)–5(d) and S6(b)–S6(d) in the supplementary material, the expected surfaces correlate well with the corresponding numerical results for elastic, shear, and bulk moduli.

As for the yield stress, it is expected that the yield stress of the hybrid structure is determined by the load, which causes the weaker structure to reach its maximum load. If two structures I (compliant) and II (stiff) with the elastic modulus and yield stress of E_I , $\sigma_{y,I}$, and E_{II} , $\sigma_{y,II}$ are combined, the ratio of the applied load sustained by the more compliant structure is $\frac{E_I}{(E_I + E_{II})} F$, where F is the total external load

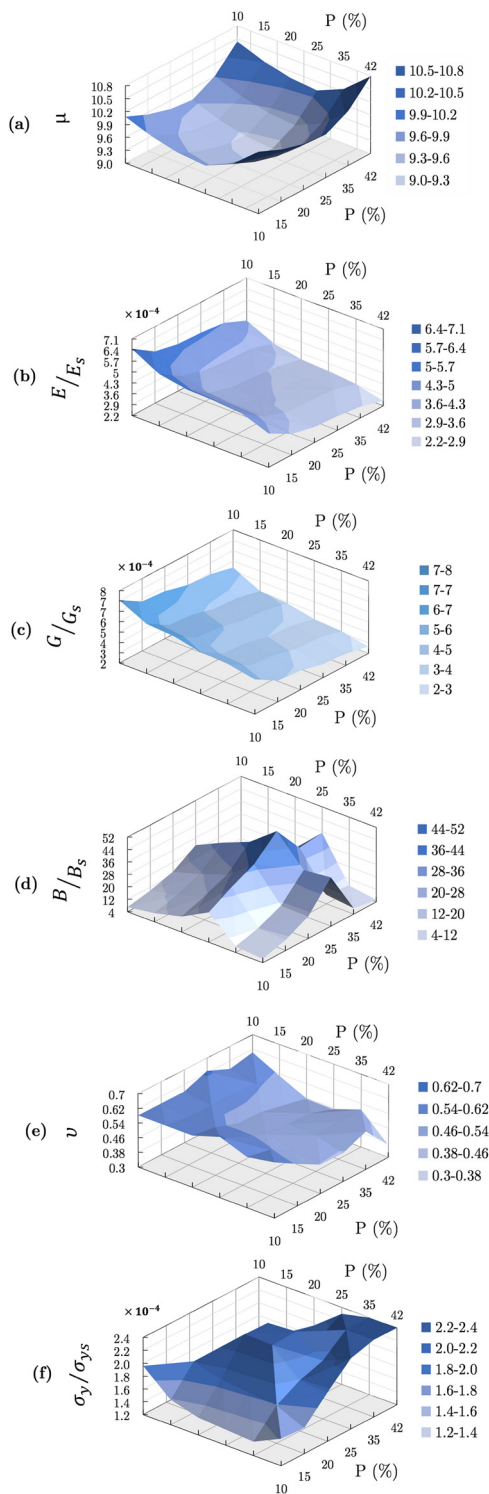


FIG. 5. Variation of (a) relative density, (b) normalized elastic modulus, (c) normalized shear modulus, (d) normalized bulk modulus, (e) Poisson's ratio, and (f) normalized yield stress of hybrid pentamode metamaterials with respect to the corresponding properties of constructing individual lattices.

applied on the structure. Therefore, the maximum stress in the compliant component in the absence and presence of the second stiff component II is $\sigma_{max,I}$ and $\frac{E_I}{(E_I+E_{II})} \sigma_{max,I}$, respectively. Therefore, the yield structure of the hybrid structure can be considered as $\sigma_y = \frac{(E_I+E_{II})}{E_I} \sigma_{y,I}$. The yield strength surface obtained from this hypothesis and the numerical yield strength surface are demonstrated in Figs. 5(d) and S6(d) in the [supplementary material](#), and as it can be seen, they have very similar topologies. The expected results are in the range of 5.58–12.04 kPa, and the numerical results are in the range of 6.08–12.8 kPa, which are very close to each other.

As for Poisson's ratio, as long as the two individual structures do not interact with each other, the lattice with higher Poisson's ratio expands greater. As the imposed strain on both individual structures is identical (and equal to that of the hybrid structure), it is expected (and later confirmed numerically) that Poisson's ratio of the hybrid structure is determined by Poisson's ratio of the individual structure with a higher Poisson's ratio value. Comparison of the expected and numerical results shows their good accordance in both topology shape and range (i.e., $0.36 < \nu < 0.63$).

In summary, the effect of varying the midpoint positioning of the pentamode structure (as a way of making pentamode anisotropic) on its mechanical properties was investigated numerically and experimentally. Moving the midpoint point along the main diagonal from the vertex to the centroid of the unit cell decreases the elastic modulus, shear modulus, and Poisson's ratio almost steadily, while in contrast, it increases yield stress steadily. The bulk modulus has a bell shape with its peak at the midpoint original position (i.e., 25% L). Hybrid intermediate pentamode lattice structures were also constructed from individual pentamode lattice structures with different B/G ratios (with the difference in B/G as large as two orders of magnitude). First and foremost, it was demonstrated that it is possible to design and construct composite intermediate extremal pentamode materials with arbitrary eigenvalues in the elastic tensor. Furthermore, it was concluded that the relative density, elastic modulus, shear modulus, and bulk modulus of the hybrid structure can be determined by the superposition of the noted properties of the individual lattice structures. The results also showed that Poisson's ratio of the hybrid pentamode structure equals that of individual structure with higher Poisson's ratio. Moreover, the yield stress of the hybrid pentamode lattice structure depends on the elastic moduli of the constructing lattice structures, as well as the yield stress of the weaker lattice structure.

See the [supplementary material](#) for the results of mesh sensitivity analysis, stress-strain curves, stress contours, tabled data of mechanical properties, and results of the constituent material.

Professor I. Shishkovsky thanks the Russian Science Foundation (Grant Agreement No. 20-19-00780) for their support.

DATA AVAILABILITY

The data that support the findings of this study are available from the corresponding author upon reasonable request.

REFERENCES

- ¹Z. G. Nicolaou and A. E. Motter, "Mechanical metamaterials with negative compressibility transitions," *Nat. Mater.* **11**(7), 608–613 (2012).

- ²R. Hedayati, M. Mirzaali, L. Vergani, and A. Zadpoor, "Action-at-a-distance metamaterials: Distributed local actuation through far-field global forces," *APL Mater.* **6**(3), 036101 (2018).
- ³T. A. Hewage, K. L. Alderson, A. Alderson, and F. Scarpa, "Double-negative mechanical metamaterials displaying simultaneous negative stiffness and negative poisson's ratio properties," *Adv. Mater.* **28**(46), 10323–10332 (2016).
- ⁴M. Kadic, T. Bückmann, R. Schittny, and M. Wegener, "On anisotropic versions of three-dimensional pentamode metamaterials," *New J. Phys.* **15**(2), 023029 (2013).
- ⁵M. Kadic, T. Bückmann, R. Schittny, P. Gumbsch, and M. Wegener, "Pentamode metamaterials with independently tailored bulk modulus and mass density," *Phys. Rev. Appl.* **2**(5), 054007 (2014).
- ⁶T. Bückmann, M. Thiel, M. Kadic, R. Schittny, and M. Wegener, "An elasto-mechanical unfeelability cloak made of pentamode metamaterials," *Nat. Commun.* **5**(1), 4130 (2014).
- ⁷R. Hedayati, A. Leeflang, and A. Zadpoor, "Additively manufactured metallic pentamode meta-materials," *Appl. Phys. Lett.* **110**(9), 091905 (2017).
- ⁸A. Rafsanjani, A. Akbarzadeh, and D. Pasini, "Snapping mechanical metamaterials under tension," *Adv. Mater.* **27**(39), 5931–5935 (2015).
- ⁹M. Kadic, T. Bückmann, N. Stenger, M. Thiel, and M. Wegener, "On the practicability of pentamode mechanical metamaterials," *Appl. Phys. Lett.* **100**(19), 191901 (2012).
- ¹⁰R. Schittny, T. Bückmann, M. Kadic, and M. Wegener, "Elastic measurements on macroscopic three-dimensional pentamode metamaterials," *Appl. Phys. Lett.* **103**(23), 231905 (2013).
- ¹¹G. W. Milton and A. V. Cherkaev, "Which elasticity tensors are realizable?," *J. Eng. Mater. Technol.* **117**(4), 483–493 (1995).
- ¹²M. Kadic, G. W. Milton, M. van Hecke, and M. Wegener, "3D metamaterials," *Nat. Rev. Phys.* **1**(3), 198–210 (2019).
- ¹³L. Zhang, B. Song, A. Zhao, R. Liu, L. Yang, and Y. Shi, "Study on mechanical properties of honeycomb pentamode structures fabricated by laser additive manufacturing: Numerical simulation and experimental verification," *Composite Struct.* **226**, 111199 (2019).
- ¹⁴A. Krushynska, P. Galich, F. Bosia, N. Pugno, and S. Rudykh, "Hybrid metamaterials combining pentamode lattices and phononic plates," *Appl. Phys. Lett.* **113**(20), 201901 (2018).
- ¹⁵Q. Li and J. S. Vipperman, "Three-dimensional pentamode acoustic metamaterials with hexagonal unit cells," *J. Acoust. Soc. Am.* **145**(3), 1372–1377 (2019).
- ¹⁶R. Hedayati, S. J. Salami, Y. Li, M. Sadighi, and A. Zadpoor, "Semianalytical geometry-property relationships for some generalized classes of pentamode-like additively manufactured mechanical metamaterials," *Phys. Rev. Appl.* **11**(3), 034057 (2019).
- ¹⁷F. Fraternali and A. Amendola, "Mechanical modeling of innovative metamaterials alternating pentamode lattices and confinement plates," *J. Mech. Phys. Solids* **99**, 259–271 (2017).
- ¹⁸A. Amendola, G. Carpentieri, L. Feo, and F. Fraternali, "Bending dominated response of layered mechanical metamaterials alternating pentamode lattices and confinement plates," *Compos. Struct.* **157**, 71–77 (2016).
- ¹⁹Y. Huang, X. Lu, G. Liang, and Z. Xu, "Pentamodal property and acoustic band gaps of pentamode metamaterials with different cross-section shapes," *Phys. Lett. A* **380**(13), 1334–1338 (2016).
- ²⁰Z. Wang, Y. Chu, C. Cai, G. Liu, and M. R. Wang, "Composite pentamode metamaterials with low frequency locally resonant characteristics," *J. Appl. Phys.* **122**(2), 025114 (2017).
- ²¹C. Cai, R. Guo, X. Wang, F. Sun, Z. Wang, and Z. Xu, "Effect of anisotropy on phononic band structure and figure of merit of pentamode metamaterials," *J. Appl. Phys.* **127**(12), 124903 (2020).
- ²²A. Amendola, C. Smith, R. Goodall, F. Auricchio, L. Feo, G. Benzonì, and F. Fraternali, "Experimental response of additively manufactured metallic pentamode materials confined between stiffening plates," *Compos. Struct.* **142**, 254–262 (2016).
- ²³K. Fishman and D. Machmer, "Testing techniques for measurement of bulk modulus," *J. Test. Eval.* **22**(2), 161–167 (1994).
- ²⁴B. Moore, T. Jaglinski, D. Stone, and R. Lakes, "On the bulk modulus of open cell foams," *Cell. Polym.* **26**(1), 1–10 (2007).